Available online at www.sciencedirect.com

SciVerse ScienceDirect

Physics Procedia 37 (2012) 773 – 780

Physics Procedia

TIPP 2011 - Technology and Instrumentation in Particle Physics 2011

A RICH detector for CLAS12 Spectrometer

Ahmed El Alaoui[1], Nathan Baltzell, Kawtar Hafidi

Argonne National Laboratory, Physics division, 9700 S. Cass Ave, Argonne IL, 60439, USA

Abstract

The upgrade of the Jefferson Lab accelerator to 12 GeV electron beam energy, combined with that of the CEBAF Large Acceptance Spectrometer (CLAS12) located in Hall B, will provide the unique combination of wide kinematical coverage, high beam intensity (luminosity), high energy, high polarization, and advanced detection capabilities required to study Quantum Chromodynamics (QCD) in greater details. A Ring Imaging Cherenkov (RICH) will significantly enhance CLAS12 particle identification capabilities by providing clean separation between pions, kaons and protons over momenta from 2 to 8 GeV/c. A detailed simulation of a preliminary design of the RICH detector for CLAS12 using GEANT-4 Monte-Carlo will be presented. A reconstruction algorithm based on a likelihood approach will be discussed.

Keywords: CEBAF, CLAS12, RICH, DRT

1. Introduction

In the past fifty years a huge effort was devoted from both experimentalists and theorists to the study of Quantum Chromodynamics (QCD). Despite the fact that many experiments have largely contributed to the understanding of this phenomenon, there are still many unexploited sectors which need high precision data to be addressed. The upgrade of the Continuous Electron Beam Accelerator Facility (CEBAF), located in Jefferson laboratory, to 12 GeV together with the upgrade of the Hall B CEBAF Large Acceptance Spectrometer (CLAS) [1] to CLAS12 will enable higher luminosity operation and improved particle identification. This will offer the unique opportunity to substantially enhance our understanding of the structure of nucleons and nuclei. Moreover, the addition of a Ring Imaging Cherenkov counter (RICH) to the existing CLAS12 detectors will make many physics programs requiring the identification of kaons feasible. A sketch of the CEBAF facility and the CLAS12 spectrometer is shown in figure 1. The latter consists of six radially symmetric sectors spanning over 20 m^2 area and covering a large solid angle. Particle identification in the forward region includes a High Threshold Cherenkov Counter (HTCC) with a pion threshold of 4.9 GeV/c, a Low Threshold Cherenkov Counter (LTCC) and a TOF scintillator array. As illustrated in table 2 the actual CLAS12 particle identification system is not sufficient to ensure complete identification and separation

[1] alaoui@anl.gov

1875-3892 doi:10.1016/j.phpro.2012.03.723

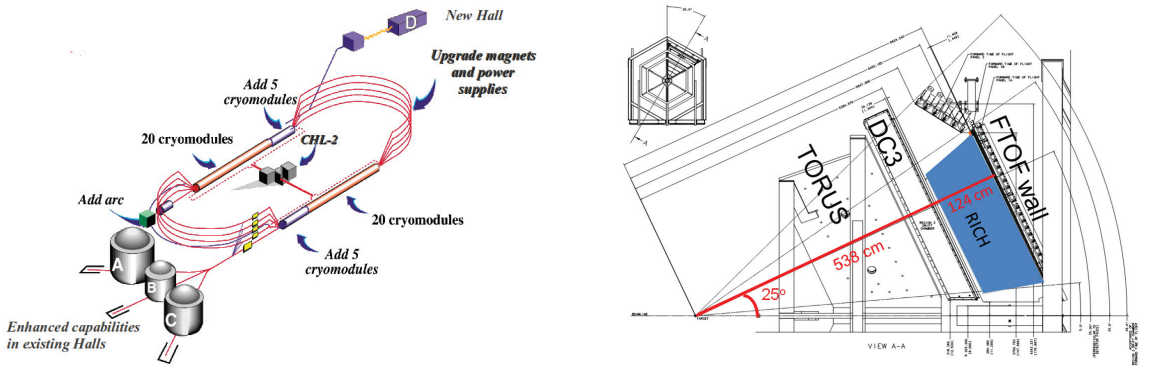

Fig. 1. Schematic view of the CEBAF facility (left) and one sector of the CLAS12 spectrometer (right). The blue band is the available space where the RICH detector will reside.

between the different hadron species in a wide momentum range. For example separation between pions and kaons in the 2.5-5 GeV/c momentum range relies solely on the performance of LTCC, and kaon-proton separation in the 4-8 GeV/c momentum range is impossible. A replacement of the existing LTCC detector with a RICH counter will greatly improve the performance of the CLAS12 spectrometer. In the following sections, detailed simulation of a RICH detector as well as a reconstruction algorithm based on a Direct Ray Tracing (DRT) method and a likelihood approach will be discussed.

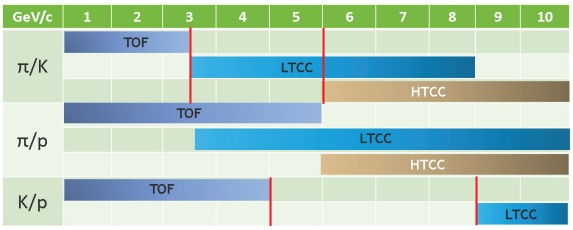

Fig. 2. Particle identification at CLAS12 provided by the TOF, the LTCC and the HTCC detectors.

2. RICH setup

A study of the RICH detector performance for CLAS12 spectrometer, based on GEANT-4 [2, 3] Monte Carlo, was carried out in order to find the best configuration for particle identification. The charged particles yield is generated using the PYTHIA[4] event generator. The angular distribution of kaons as function of momentum is plotted in figure 3. The RICH detector has to fulfill some requirements. It should have a relatively small depth to fit inside the available 124 cm space (figure 1 (right)), it should operate in a high rate environment and in the presence of an intense magnetic field, it should have a reasonable cost and finally it should not have a significant impact on the performance of the other CLAS12 components, especially the Time-of-Flight detector located downstream the RICH. A proximity focusing RICH similar to the one used in hyper-nuclear spectroscopy experiment in Hall A [5, 6] in Jefferson lab was chosen as a starting point because it offers reasonable performance and cost. It consists of a liquid freon radiator (C_6F_{14}) with a refractive index n=1.28 and a thickness of 15 mm, a 5 mm thick quartz window and a proximity gap filled with CH_4 gas. The Cherenkov photons are converted into electrons via a thin layer of CsI material deposited on an array of 8×8 mm^2 pads that represent the cathode of the Multi-Wire-Proportional-Chamber (MWPC). The goal from this study is to optimize the detector parameters: the radiator thickness, the refractive index,

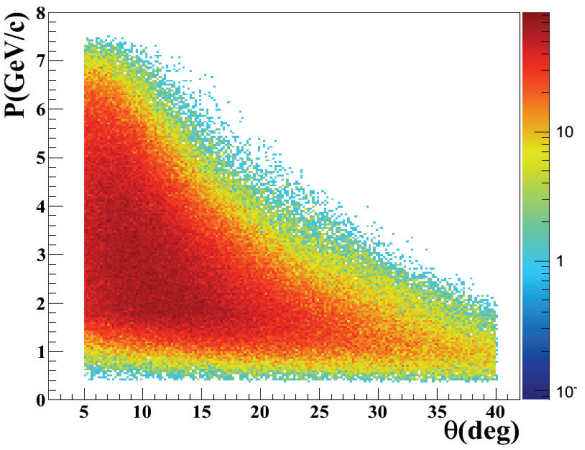

Fig. 3. Angular distribution of kaons as function of momentum produced from semi inclusive deep inelastic scattering process. The distribution is obtained from PYTHIA event generator.

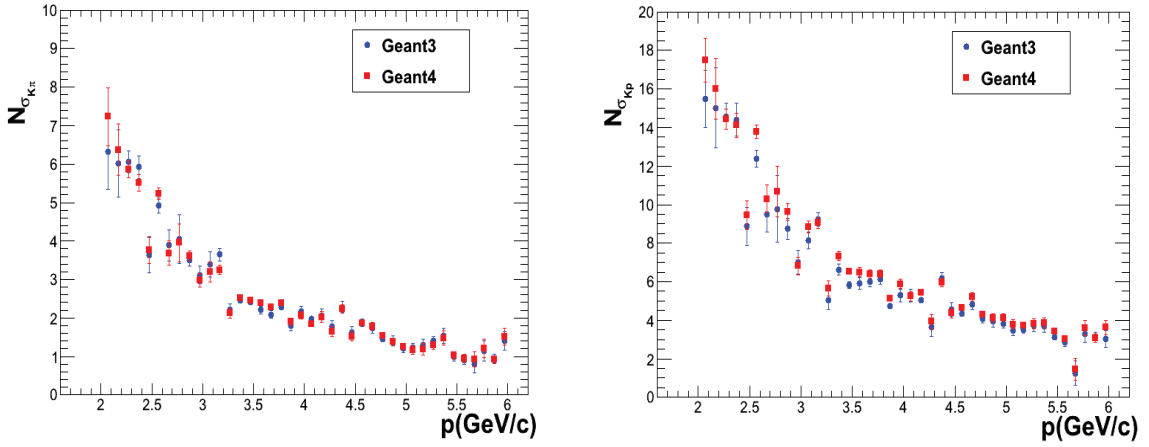

Fig. 4. N_σ separation for pion-kaon (left) and kaon-proton (right) as function of charged particle momentum. Those numbers were obtained from two independent simulations using GEANT-3 (blue solid circle) and GEANT-4 (red solid square) toolkits.

the gap thickness, the detector pad size. The outcome of this study is given in terms of the separating power (N_σ) and the number of photoelectrons (N_{pe}) defined by [7]

$$N_\sigma = \frac{m_1^2 - m_2^2}{2\,\sigma_{\theta_C}\,p^2\,\sqrt{n^2-1}} \tag{1}$$

and,

$$N_{pe} = L\,N_0\,sin^2\,\theta_C. \tag{2}$$

where $m_{1,2}$ (p) are the masses (momentum) of the charged particle, σ_{θ_C} is the Cherenkov angle resolution, n is the radiator index of refraction, L is the gap length and $N_0 = (\alpha/\hbar\,c)\int QTR\,dE$ is the detector response parameter. It includes the detector quantum efficiency (Q), the radiator transmittance (T) and eventually the mirror reflectivity (R). Two independent simulations were performed separately to evaluate the pion-kaon and kaon-proton separating powers. The results are presented in figure 4. They show first that both analysis agree with each other and second that the use of a C_6F_{14} liquid radiator and CsI photocathode for

photon detection did not provide enough separation between kaons and pions for momentum larger than 3 GeV/c. An alternative solution would be to replace the liquid radiator by a silica aerogel and the CsI

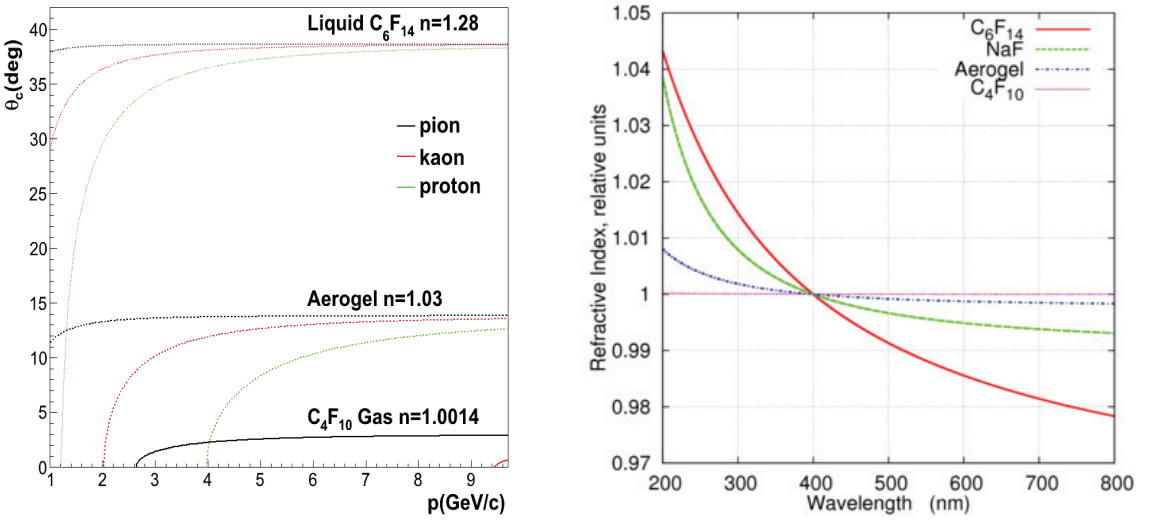

Fig. 5. (left panel): Cherenkov angle as function of charged particle momentum for pions (black), kaons (red) and protons (green) and for aerogel, C_4F_{10} gas and C_6F_{14} liquid radiators. (right panel): Dispersion of aerogel as function of photon wavelength compared to sodium fluoride (NaF), liquid C_6F_{14} and gas C_4H_{10} radiators.

photocathode by photomultipliers. The CsI photocathode has a small quantum efficiency in the visible light

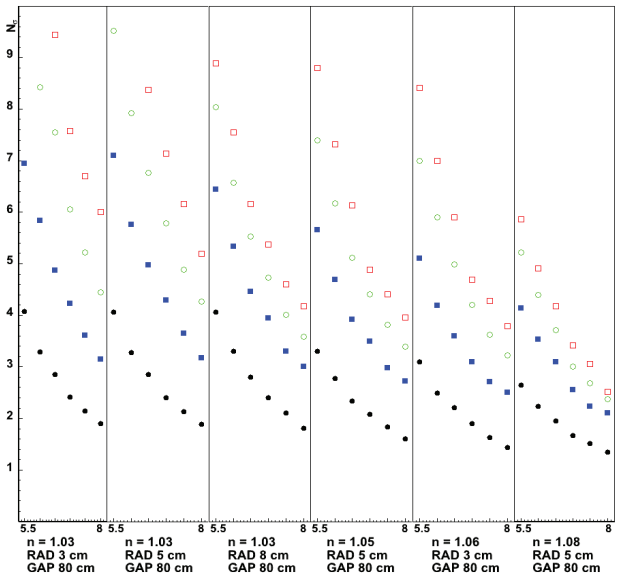

Fig. 6. pion-kaon separating power, N_σ, as function of charged particle momentum for different radiator thickness and refractive index. The different data points correspond to different detector pad sizes: open square(circle) and solid square(circle) represent respectively a pad size of 0.3×0.3 cm^2(0.6×0.6 cm^2) and 1.0×1.0 cm^2(2.0×2.0 cm^2). See text for explanation of the data.

region so it is inadequate to use it with aerogel. As shown in figure 5 (right), aerogel has a small dispersion especially in the visible range compared to other type of radiators. This characteristic is very important

because it reduces effects related to chromatic aberration which have a large contribution to the Cherenkov angle uncertainty. An other point behind using aerogel is shown in figure 5 (left). This material offers a clear separation between different hadron species in the whole 2-8 GeV/c momentum range, while liquid (gas) radiators are good for separation between particles having low (high) momentum only. The study is

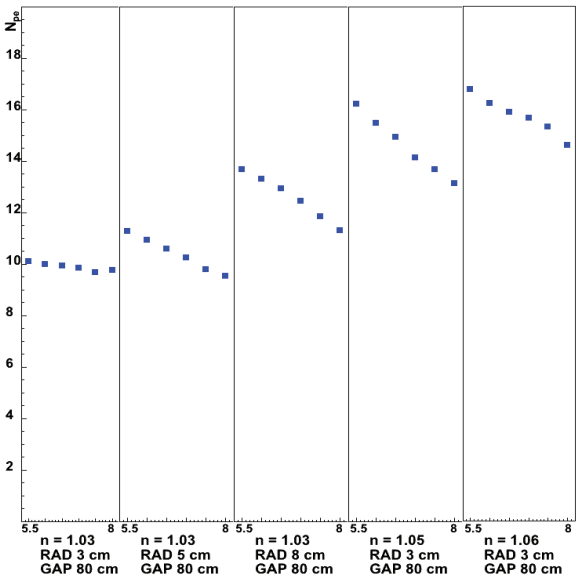

Fig. 7. Number of photoelectrons, N_{pe}, as function of momentum for different radiator thickness and refractive index. Here The pad size is 1×1 cm^2 and the gap length is 80 cm.

then repeated again using aerogel instead of liquid C_6F_{14} and PMTs instead of MWPC. Preliminary results of the simulation are summarized in figures 6 and 7. Each column on both plots shows respectively the pion-kaon separating power (N_σ) and the number of photoelectrons (N_{pe}) as function of momentum for a given configuration. Each set of data points in figure 6 corresponds to different detector pad size. The result shows that increasing the radiator thickness decreases N_σ but only for small pad size. Increasing the refractive index reduces N_σ but on the other hand increases N_{pe}. An ideal configuration has to maximize both N_σ and N_{pe} at the same time but usually a compromise has to be found. The study shows also that increasing the gap length increases N_σ. Keeping in mind space limitation, an 80 cm length gap was chosen. The optimized parameters obtained from this simulation are listed in table 1. The Hamamatsu H8500 64 channels multi-anode PMTs

n	1.03
Aerogel thickness	3 cm
Gap thickness	80 cm
Detector pad size	1.0×1.0 cm^2

Table 1. RICH detector parameters that offer the best performance.

Dimension	Effective area	Pixel size	packing factor	quantum efficiency	band width
52×52×28 mm^3	49×49 mm^2	6×6 mm^2	89%	30%	260-650 nm

Table 2. Characteristics of the Hamamatsu H8500 64 channels multi-anode PMT.

are chosen as photon detector because they have an excellent packing factor and a high quantum efficiency

in the visible region range. Their characteristics are shown in table 2. Unfortunately such configuration will have a very high cost due to the large number of PMTs needed to cover the whole geometrical acceptance. To overcome this issue, a system of dual mirrors which consists of an ellipsoid mirror and a planar mirror will be used to focus the Cherenkov photons on a small area. In this scenario two kind of detections are considered. The first one is called direct detection for the very forward particles emerging with polar angles smaller than 12 degree. The second detection is referred to as inward reflection detection for particle emerging with polar angles in the 12-35 degree range. In the second case the photons have to be reflected twice and go through the radiator twice before reaching the detector. This will reduce the total number of PMTs by a factor of 3 but on the other hand will reduce the number of photoelectrons by a factor of 4. This is an ongoing simulation and preliminary results look promising. A downstream view of the RICH detector for the six sectors is depicted in figure 8. The impact of the RICH detector material on TOF performance is also studied using the CLAS12 GEMC toolkit[8]. Differences in TOF measurements with and without the inclusion of the RICH inside the CLAS12 spectrometer for different particles are simulated. The large difference is found to be around 20 ps which is below the 120 ps TOF resolution leading to the conclusion that the effect of the RICH material on the TOF performance is negligible.

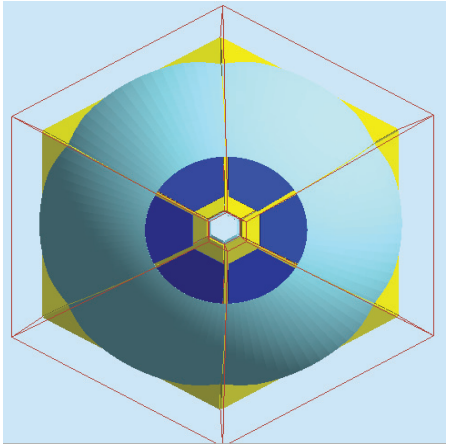

Fig. 8. Downstream view of the RICH detector for the six sectors. The aerogel radiator is shown in yellow, the ellipsoid mirror is shown in cyan and the PMT plane is shown in blue. The planar mirror, not shown here, is located upstream the PMT plane.

3. Reconstruction algorithm

A reconstruction algorithm based on Direct Ray Tracing (DRT) and likelihood approach is used in order to determine the type of the particle that produces a ring in the RICH detector. It combines information on the charged particle momentum and the hits recorded in the photon detector to calculate a hit probability distribution for the PMTs. For each charged track t with momentum p, and for each mass hypothesis h, a large number of photons, $N_{PE}^{h,t}$, is generated and propagated towards the photon detector plane. Let $P^{h,t}(i) = N_{PE}^{h,t}(i)/N_{PE}^{h,t}$ be the probability that the i-th PMT is struck by a photon. When evaluating this probability, the aerogel transmittance, the mirror reflectivity, the geometry packing factor, the detector quantum efficiency, and the PMT pad size are taken into account. Assuming the photoelectrons have a Poisson distribution, the probability that the i-th PMT responds is given by

$$P_{PMT}^{h}(i) = \exp(-N_{PE}^{h}(i) - B_{PE}^{h}(i)) \tag{3}$$

where $B_{PE}^{h}(i)$ is a background term.
The likelihood that a particle produce a ring in the detector plane can be expressed by

$$L(h,t) = \sum_{i} \log\left\{P_{PMT}(h,t,i)\, C_{PMT}(i) + \bar{P}_{PMT}(h,t,i)\,(1 - C_{PMT}(i))\right\} \tag{4}$$

where $\bar{P}_{PMT}(h,t,i) = 1 - P_{PMT}(h,t,i)$. The coefficients $C_{PMT}(i)$ are either 1 or 0 depending whether or not the i-th PMT is part of the measured hit distribution. Since experimental data is not available yet, a simulation which combines PYTHIA event generator and GEANT-4 toolkit is used to determine the coefficients $C_{PMT}(i)$. The hypothesis h that maximize $L(h,t)$ is considered as the true particle type. Figures 9 and 10 show the normalized likelihood as function of particle momentum for pions, kaons and protons respectively for the direct detection and the inward reflection detection cases. The results are presented in a matrix form. The diagonal elements are the likelihood that the particle is really of true type t and the off-diagonal elements represent the probability to misidentify the true particle type. Note that the rows must add up to unity. The method seems to work perfectly for both detection case except for some cases where the ring is not completely included in the detector plane due to geometrical limitations.

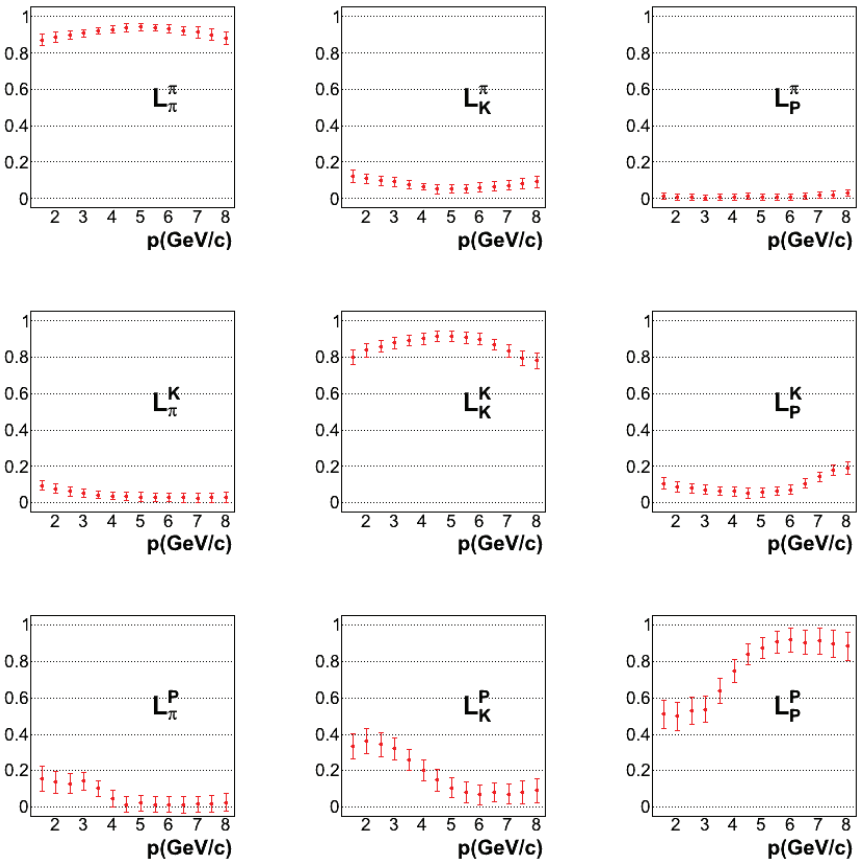

Fig. 9. Normalized likelihood for pions, kaons and protons as function of momentum in case of direct detection. The diagonal plots represent the probability to identify a pion as a pion (top), a kaon as a kaon (middle) and a proton as a proton (bottom). The off-diagonal plots are the misidentification probabilities.

4. conclusion

In this paper a detailed simulation for a RICH detector for CLAS12 spectrometer was presented. The combination of aerogel radiator, a dual mirrors system and the Hamamatsu H8500 64 channels multi-anode PMTs offer an adequate choice for hadron detection. Particle identification is obtained through a reconstruction algorithm which converts the hits recorded in the PMTs into a probability distribution for each charged particle type. Proof of principle results look very encouraging and show that the RICH detector is capable

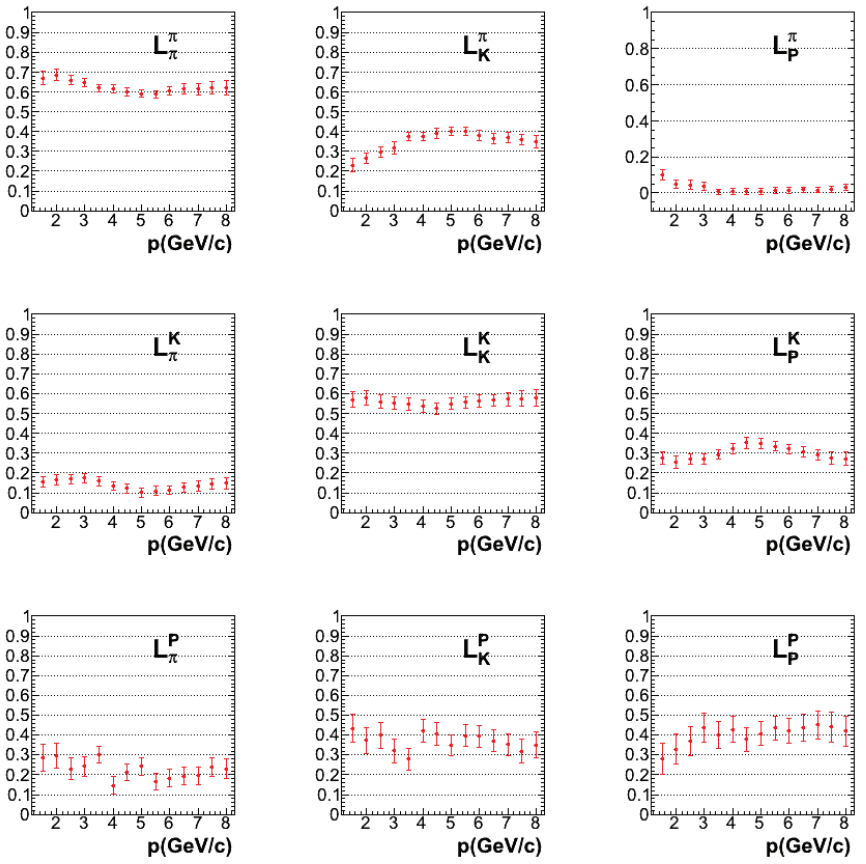

Fig. 10. Normalized likelihood for pions, kaons and protons as function of momentum in case of inward reflection detection. The diagonal plots represent the probability to identify a pion as a pion (top), a kaon as a kaon (middle) and a proton as a proton (bottom). The off-diagonal plots are the misidentification probabilities.

to identify and separate between hadron species in a wide momentum range with a high efficiency and low contamination. More details are being worked out with future simulations.

Acknowledgments

This work is supported by the U.S. Department of Energy, Office of Nuclear Physics, under contract No. DE-AC02-06CH11357.

References

[1] B. A. Mecking, et al., The cebaf large acceptance spectrometer (clas), Nucl. Instrum. Meth. A 503 (2003) 513–553.
[2] S. Agostinelli, et al., Geant4– a simulation toolkit, Nucl. Instrum. Meth. A 506 (2003) 250–303.
[3] J. Allison, et al., Geant4 developments and applications, IEEE Trans. Nucl. Sci. 53 (2006) 270–278.
[4] T. Sjostrand, et al., Pythia 6.4 physics and manual, JHEP 05 (2006) 1–581.
[5] F. Garibaldi, et al., A proximity focusing rich detector for kaon physics at jefferson lab hall a, Nucl. Instrum. Meth. A 502 (2003) 117–122.
[6] M. Iodice, et al., Performance and results of the rich detector for kaon physics in hall a at jefferson lab, Nucl. Instrum. Meth. A 553 (2005) 231–236.
[7] T. Ypsilantis, J. Seguinot, Theory of ring imaging cherenkov counters, Nucl. Instrum. Meth. A 343 (1994) 30–51.
[8] Geant4 monte carlo for clas12, `https://gemc.jlab.org/gemc/Home.html`.